Ann. Geophys., 27, 373–379, 2009
www.ann-geophys.net/27/373/2009/

Annales Geophysicae

Rayleigh lidar observations of enhanced stratopause temperature over Gadanki (13.5° N, 79.2° E) during major stratospheric warming in 2006

S. Sridharan[1], **S. Sathishkumar**[2], **and K. Raghunath**[1]

[1]National Atmospheric Research Laboratory, Gadanki-517 112, Pakala Mandal, Chitoor, India
[2]Equatorial Geophysical Research Laboratory, Indian Institute of Geomagnetism, Krishnapuram, Tirunelveli-627 011, India

Received: 12 August 2008 – Revised: 4 December 2008 – Accepted: 16 December 2008 – Published: 22 January 2009

Abstract. Rayleigh lidar observations of temperature structure and gravity wave activity were carried out at Gadanki (13.5° N, 79.2° E) during January–February 2006. A major stratospheric warming event occurred at high latitude during the end of January and early February. There was a sudden enhancement in the stratopause temperature over Gadanki coinciding with the date of onset of the major stratospheric warming event which occurred at high latitudes. The temperature enhancement persisted even after the end of the high latitude major warming event. During the same time, the UKMO (United Kingdom Meteorological Office) zonal mean temperature showed a similar warming episode at 10° N and cooling episode at 60° N around the region of stratopause. This could be due to ascending (descending) motions at high (low) latitudes above the critical level of planetary waves, where there was no planetary wave flux. The time variation of the gravity wave potential energy computed from the temperature perturbations over Gadanki shows variabilities at planetary wave periods, suggesting a non-linear interaction between gravity waves and planetary waves. The space-time analysis of UKMO temperature data at high and low latitudes shows the presence of similar periodicities of planetary wave of zonal wavenumber 1.

Keywords. Atmospheric composition and structure (Pressure, density, and temperature) – Meteorology and atmospheric dynamics (Middle atmosphere dynamics; Waves and tides)

Correspondence to: S. Sridharan
(ssri_dhar@rediffmail.com)

1 Introduction

A sudden stratospheric warming event is a dramatic event of the high latitude middle atmosphere which involves sudden change of temperature, wind and circulation (Matsuno, 1971; Andrews et al., 1987) and has been observed at mid- (Hauchecorne and Chanin, 1983) and high latitudes (Whiteway and Carswell, 1994; Whiteway et al., 1997; Duck et al., 1998; Walterscheid et al., 2000). They are classified as a major event, if the zonal-mean temperature increases poleward from 60° latitude at 10 hPa or below, with an associated circulation reversal and hence a breakdown or splitting of the polar vortex and minor event, if the temperature increase is accompanied by no reversal of mean zonal winds at the 10 hPa level (Labitzke and Naujokat, 2000). If a major warming event occurs, it usually takes 4–6 weeks for the zonal mean circulation to return to the pre-warming state (Schoeberl, 1978). The dynamical mechanisms responsible for sudden warmings involve upward propagation of transient planetary (Rossby) waves from the troposphere into the stratosphere where they undergo critical level interaction with the mean flow and transport of westward momentum (Matsuno, 1971). Vortex dynamics is another mechanism suggested for the formation of this phenomenon (O'Neil and Pope, 1988; Shephered et al., 2000). If the vortex moves off the pole then we have a wave-1 warming; if it splits in two, then we have a wave-2 warming. The cause of such warming have also been interpreted in terms of gravity wave (GW) activity (Whiteway and Carswell, 1994; Whiteway et al., 1997). Whiteway and Carswell (1994) observed greater dissipation of gravity wave energy within the upper stratospheric warming at high latitudes in comparison to the preceding and following periods. The warming events include cooling of a few degrees in the mesosphere (Schoeberl, 1978; Appu, 1984; Delisi and Dunkerton, 1988; Duck et al., 1998;

Published by Copernicus Publications on behalf of the European Geosciences Union.

Walterscheid et al., 2000). The mesospheric cooling and deceleration/ reversal of the mesospheric zonal wind at high winter latitudes were observed several days before the onset of the major warming event in the stratosphere (Walterscheid et al., 2000; Dowdy et al., 2004). Using 35 years of data, Dunkerton et al. (1988) found that the occurrence of major warming events depends on the equatorial Quasi-Biennial Oscillation (QBO) phase. In particular, they showed that major warming events did not occur, when the QBO winds are in deep eastward phase.

Siva Kumar et al. (2004) examined the stratospheric warming effects at low latitudes employing Rayleigh lidar temperature observations from Gadanki (13.5° N, 79.2° E). They reported a stratospheric warming event at low latitudes about a week after a major stratospheric warming was registered at high latitudes, with a temperature increase of 18 K above the tropical winter mean values at 45 km height.

Here we present Rayleigh lidar temperature observations over Gadanki during January–February 2006. The daily temperature and gravity wave variabilities are discussed in connection with major stratospheric warming event occurring at high latitudes. The NCEP zonal mean and temperature data are used to identify the major warming event. In addition, the daily UKMO temperature data are used to infer the presence of planetary waves at 10° N and 60° N.

2 Observations and data analysis

2.1 Rayleigh lidar temperature data

Rayleigh lidar, installed at Gadanki under Indo-Japanese collaboration, has been operated during nighttime under cloud free conditions since March 1998. The lidar employs a Nd:YAG laser, which operates at the second harmonic wavelength of 532 nm. The pulse energy is 550 mJ and pulse width is 7 ns. The lidar is operated with an altitude resolution of 300 m and pulse repetition frequency of 20 Hz. The system provides backscattered signals, which are integrated over 5000 transmitted pulses corresponding to a temporal averaging of 250 s. The temperature information is retrieved from the received photon counts using the method adopted by Hauchecorne and Chanin (1980). There have been quite a number of results reported from this site (Bhavani Kumar et al., 2000; Parameswaran et al., 2000; Siva Kumar et al., 2001, to state a few). Though the highest altitude is taken as 90 km and from which temperature is derived using downward integration, the standard error in the estimation of temperature information above 75 km is larger and hence the data for the heights 30 and 75 km are only presented. The lidar operation limits to nighttime and cloud free conditions and hence the data for each night also varies. The Rayleigh lidar observations have been carried out in almost all the nights during January–February 2006. As the major stratospheric warming event occurred at high latitudes during end of January 2006, the temperature observations over Gadanki provide us the opportunity to examine thermal structure and gravity variabilities at low latitudes prior to, during and after the major stratospheric warming event occurring at high latitudes. The temperature profiles derived for every half an hour and the temperature perturbations $T'(z)=T(z)-T_o(z)$ are extracted from the half-hour averaged profiles. The background temperature profile ($T_o(z)$) is obtained by averaging the temperature profile for the entire night and smoothed vertically by 5 km. The root-mean-square (rms) perturbation and available potential energy per unit mass are used to infer whether there was dissipation of energy. At a given altitude, the variance of temperature perturbation from the estimated background state was computed from the series of half-hour average temperature profiles obtained on a given night. The noise variance due to statistical uncertainty in the photon counting process is subtracted to obtain real atmospheric temperature fluctuations, which at a given altitude is given by

$$\overline{\left(\frac{T'(z)}{T_0(z)}\right)_r^2} = \frac{1}{N_P}\sum_{i=1}^{Np}\left(\frac{T'(z)}{T_0(z)}\right)_i^2 - \frac{1}{N_P}\sum_{i=1}^{Np}\left(\frac{\delta T(z)}{T_0(z)}\right)_i^2$$

where $\delta T(z)$ is the uncertainty in the temperature measurement at height z due to statistical fluctuations in the photon counting process. The real variance is then used to determine a profile of rms perturbation and also the average available potential energy per unit mass $Ep(z)=\frac{1}{2}\left(\frac{g}{N(z)}\right)^2\overline{\left(\frac{T'(z)}{T_0(z)}\right)_r^2}$, where $N(z)$ is the brunt-vaisala frequency and g is acceleration due to gravity. The temperature derivative is used to obtain $N(z)$, which is computed by using three adjacent points.

2.2 UKMO data

We have also used stratospheric fields of daily (at 12:00 UTC, Coordinated Universal Time) zonal mean temperature, and zonal and meridional wind components provided by the UK Meteorological Office (UKMO) from the British Atmospheric Data Centre (BADC) website at http://badc.nerc.ac.uk. These data have global coverage with 2.51 latitudinal and 3.751 longitudinal steps and are available at 22 pressure levels from 1000 hPa to 0.316 hPa (0–55 km) with a 1-day temporal resolution (Swinbanks and O'Neill, 1994a; Swinbank and Ortland, 2003). In the current study, we employ the zonal wind and temperature data at 10 hPa, 1 hPa and 0.5 hPa over 10° N and 60° N for the period December 2005–February 2006.

2.3 NCEP data

The NCEP Re-analysis project has been providing the temperature and wind information from ground to lower stratosphere at intervals of about 2.5×2.5 latitude and longitude resolution (Kalnay et al., 1996). The daily stratosphere temperature and zonal winds at 10 hPa and 30 hPa for the period

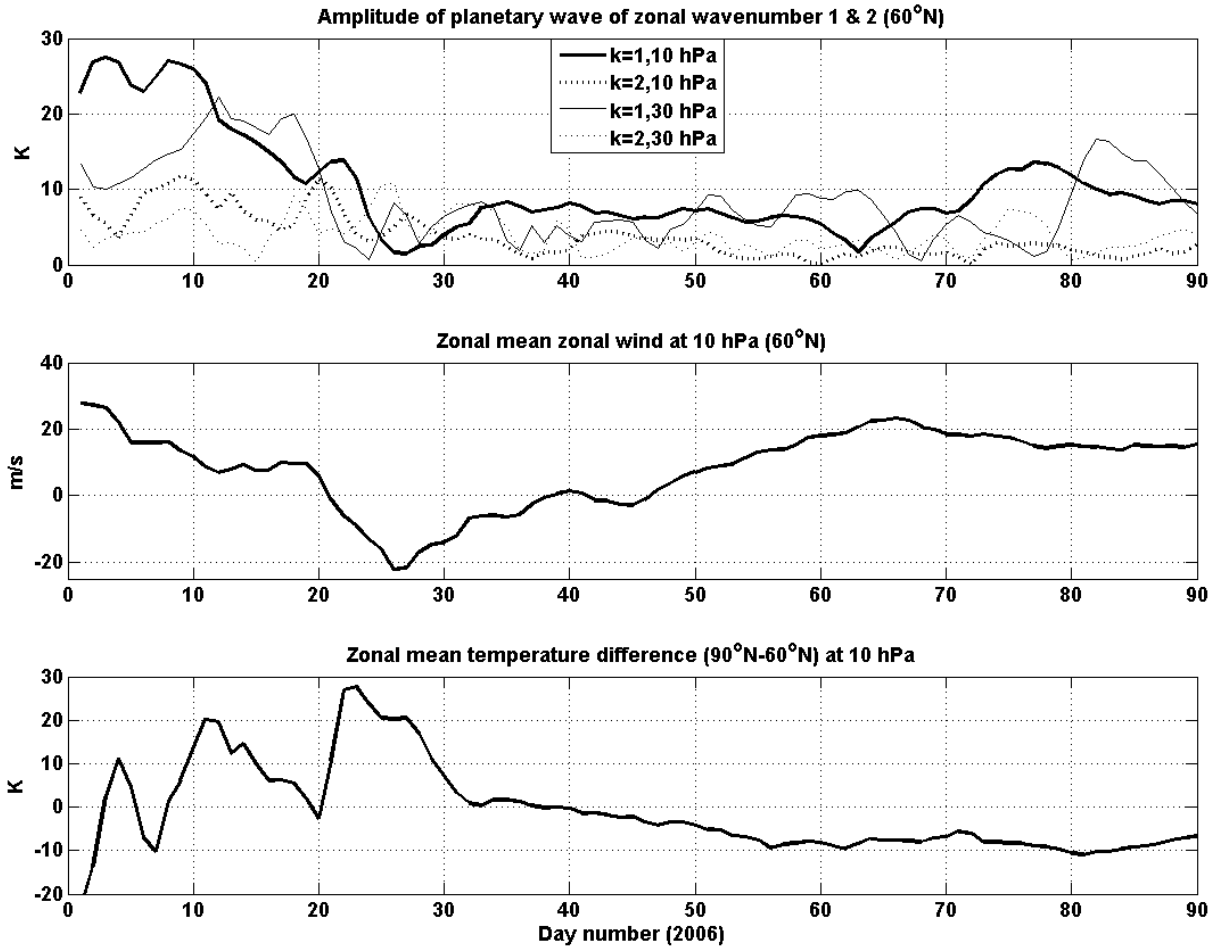

Fig. 1. The stratospheric winter 2006 (top) amplitudes of planetary waves of zonal wavenumbers 1 and 2 at 30 hPa and 10 hPa; (middle) zonal mean wind (60° N); and (bottom) temperature difference (90° N–60° N) at 10 hPa.

January–March 2006 are used to identify the duration of sudden stratospheric warming.

3 Results

The state of the winter stratosphere at 10 hPa and 30 hPa is presented using NCEP zonal mean temperature and zonal wind data in Fig. 1. The bottom panel of the Fig. 1 shows the NCEP temperature difference between the latitudes 90° and 60° N. There are series of warming events, which can be inferred from the positive temperature difference on days 3–5, 8–19, 20–33. These warming events can be classified as major or minor depending on whether there is any wind reversal at latitude 60° N. Though there are three successive warming events, only the third event is the major warming event, as it is accompanied by the reversal of zonal winds from eastward to westward. The westward winds persist during day numbers 21–38. As done by Hoffmann et al. (2007) for geopotential height, the time variation of the amplitude of planetary wave of zonal wavenumbers (k) 1 and 2 at 10 hPa and 30 hPa is shown in the top panel of Fig. 1. It can be inferred from the figure that the wave at 10 hPa is enhanced several days before the major warming event, coinciding with minor warming events. The wave amplitudes reduce drastically at the time of onset of the major warming event. The enhanced planetary wave activity leads to an upward and poleward directed heat flux connected with a reversal of the stratospheric circulation and to the strong reversals of the meridional temperature gradients (Andrews et al., 1987). The major warming is usually accompanied by cooling of the polar mesosphere and low-latitude stratosphere.

The thermal structure low-latitude middle atmosphere preceding, during and after the major stratospheric warming period is investigated. Figure 2 shows daily averaged Rayleigh lidar temperature measurements over Gadanki (13.5° N, 79.2° E). There is a sudden increase of temperature at stratopause heights on day number 21, coinciding with the major warming event occurring at high latitude. The difference between mean temperature of day numbers 5–15 and 25–35 is 5–10°K in the height region 45–50 km. The

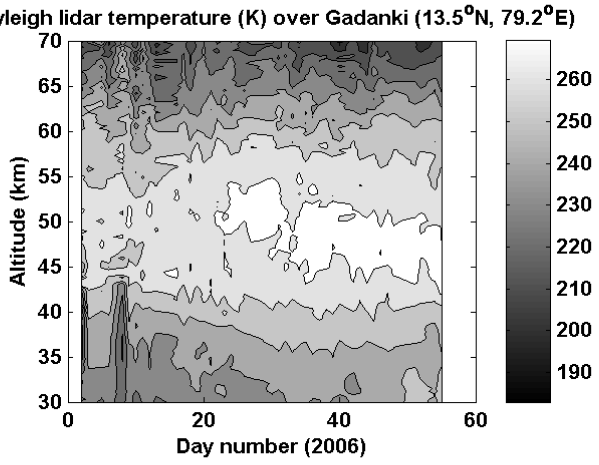

Fig. 2. Daily averaged Rayleigh lidar temperature over Gadanki (13.5° N, 79.2° E).

maximum temperature in the daily averaged temperature profile on day number 20 is 267 K and is increased to 280 K on day number 25 and nearly maintains a temperature of 275 K until the end of the observation period. The increased temperature maintains even after day number 33, when the major warming event ends at high latitude. The lower mesosphere (70–75 km) region experiences significant cooling of nearly 20°K. Changes in wind speed and direction during a sudden stratospheric warming will inhibit the upward propagation of gravity waves and lead to a cooling towards radiative equilibrium in the mesosphere (Lindzen, 1981; Holton, 1983; Dunkerton and Butchart, 1984). Whiteway and Carswell (1994) observed mesospheric cooling at high latitude site Eureka (80° N, 86° W) during the sudden stratospheric warming event.

In order to see the latitudinal structure of temperature and winds, UKMO zonal mean temperature and zonal winds are considered. Figure 3 shows the daily variation of UKMO zonal mean temperature difference between the latitudes 60° N and 90° N, zonal mean zonal wind at 60° N, zonal mean temperature and zonal mean zonal wind at 10° N. The three warming events can also be inferred from UKMO data sets. All three warming events persist almost entirely in the stratosphere. The third event, which is a major warming event, is accompanied by the reversal of zonal mean zonal wind at 60° N. The reversal first begins at mesospheric heights and slowly descends down to stratosphere. At 10° N, the zonal mean zonal wind shows eastward winds at stratospheric heights throughout January–February 2006. However, at mesospheric heights, westward winds are observed prior to the onset of major warming events and they decelerate slowly, after the onset of a major warming event at high latitudes. Above the major warming event, with the onset at day number 21, the zonal mean temperature difference is reversed at high latitude and the reversed temperature difference persists in the region around 1 hPa even during the end of February. Coinciding with this cooling episode at high latitudes, warming episode occurs at low latitudes and is consistent with the Rayleigh lidar observations over Gadanki.

Figure 4 shows the time variation of potential energy per unit mass averaged over the heights 50–60 km (top panel), 40–50 km (middle panel) and 30–40 km (bottom panel). Before the onset of warming vents, the E_p values are larger at all heights. The values decrease drastically just before the onset of the event. The E_p values for the heights 30–40 km and 50–60 km show similar time variation during the day numbers 1–25. The E_p values are larger (50–70 J/kg) on day number 16 and they decrease drastically to 7–12 J/kg on day number 21. However, E_p values for the height region 40–50 km show a sudden increase (∼40 J/kg) two days prior to the onset of the warming event at high latitudes, but decrease drastically to ∼7 J/kg in two days. The variation of E_p values seems to show modulation at periods in the range of 7–25 days. It could probably be due to the interaction of planetary waves with gravity waves. In order to identify the dominant planetary wave periods, by which the potential energy gets modulated, Lomb-Scargle periodogram is applied to the daily averaged E_p. Figure 5 shows the Lomb-Scargle periodogram of E_p values for the heights 50–60 km (curve with solid squares), 40–50 km (curve with open circle) and 30–40 km (curve with triangles). Strong peaks can be observed predominantly at periods near 25 days, 12–15 days and 7-day at all the height regions. These planetary waves develop in the troposphere, propagate vertically into the stratosphere along the axis of the jet core, and eventually bend towards the tropics. The wave decelerates the polar night jet by depositing westward momentum into the eastward jet.

In order to see the existence of those planetary waves in temperature, the UKMO temperature data for the pressure levels at 10 hPa, 1 hPa, and 0.5 hPa are considered. The spectrum of planetary wave of zonal wavenumber 1 in UKMO temperature data at 60° N (top panel) and 10° N (bottom panel) is shown in Fig. 6 for the period December 2005–February 2006. The spectrum clearly shows the presence of westward propagating waves having periods 16–20 days and 8–12 days at 60° N. Westward propagating waves having periods in the range 7-15 days have been observed at low-latitudes at 1 hPa. The 16–20 day wave observed at 60° N at 10 hPa does not appear at 10° N. From the Fig. 5, we have inferred that the gravity wave potential energy largely gets modulated by the planetary wave periods near 16 and 20 days. The reduced amplitude of the wave at 10° N at the pressure level 10 hPa could be due to its non-linear interaction with gravity waves.

4 Discussion and conclusions

This paper presents temperature and gravity wave variabilities during the period January–February 2006, which

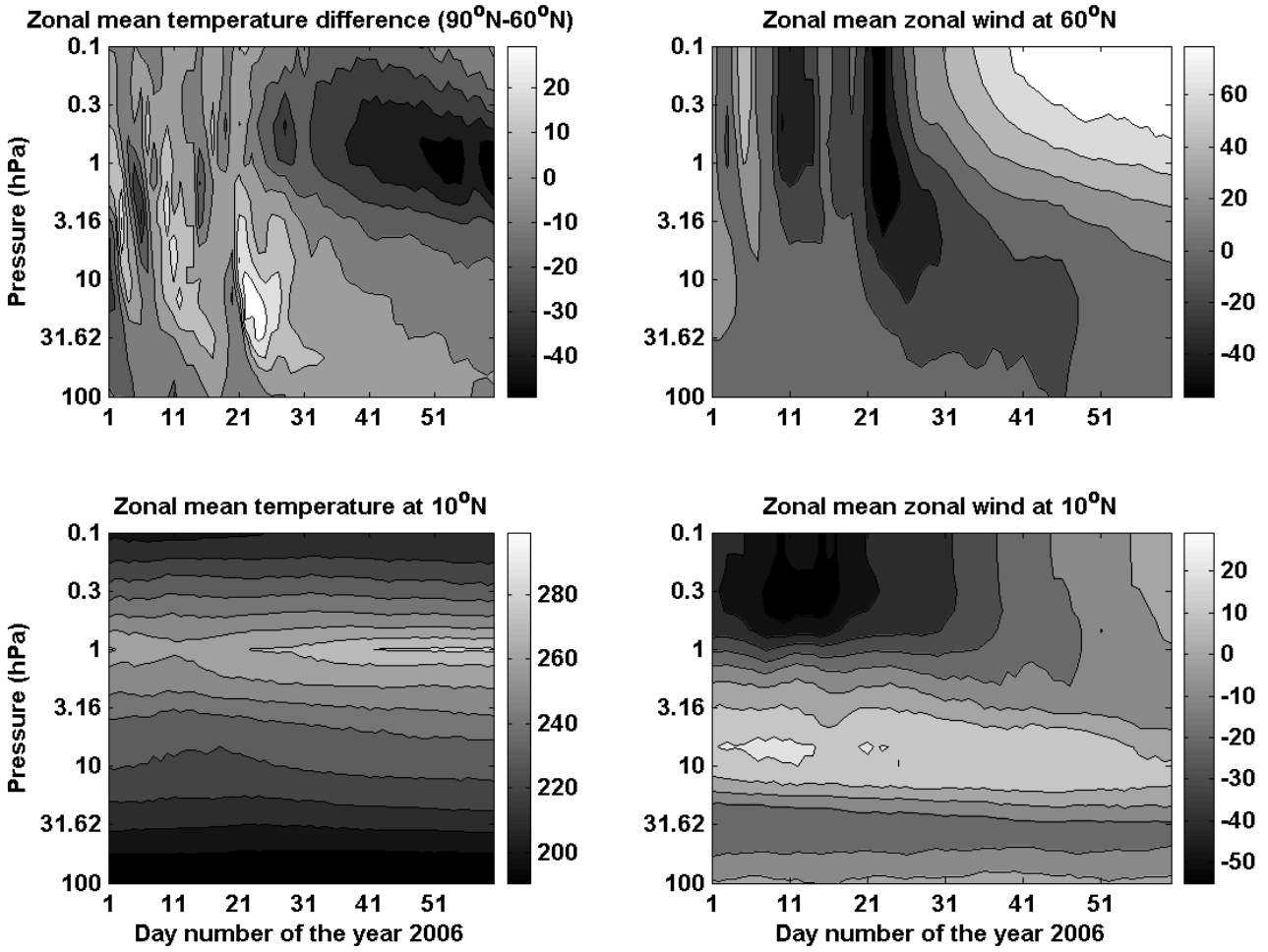

Fig. 3. UKMO data: (top left) Daily variation of zonal mean temperature difference (90° N–60° N), (bottom left) zonal mean zonal wind at 60° N, (top right) zonal mean temperature and (bottom right) zonal mean zonal wind at 10° N.

includes the period of major warming event occurred at high latitudes. The stratopause temperature over the low latitude site, Gadanki (13.5° N, 79.2° E) suddenly increases on the onset date of the sudden stratospheric warming event occurring at high latitudes. Earlier, Siva Kumar et al. (2004) presented an increase in stratopause temperature by 18 K with respect to the winter-mean temperature profile derived from the lidar data collected during March 1998 to July 2001. Because of the data gaps, they could identify the warming event two weeks after the onset of major warming event at high latitudes. The present study reports the enhancement of stratopause temperature simultaneously with the warming event at high latitude lower stratosphere. The stratopause warming over Gadanki persists even after the end of the high latitude warming event. This effect clearly demonstrates a strong latitudinal coupling of the thermodynamic processes in the upper stratosphere/lower mesosphere during the major stratospheric warming event. The gravity wave potential energy per unit mass computed from the temperature perturbations show large day to day variabilities. They seem to be modulated at periods of planetary waves. The spectrum of planetary waves of zonal wavenumber 1 in UKMO temperature shows similar periodicities, as shown by spectrum of gravity wave potential energy. This suggests the non-linear interaction of gravity waves and planetary waves. Siva Kumar et al. (2004) made Eliassen-Palm (E-P) flux calculations from ECMWF analysis showing evidence of propagation of planetary-wave activity from high and mid- to low latitudes subsequent to the major warming episode over the pole. They suggested that the observed stratopause warming could be due to the increase in planetary-wave activity. Generally, upward propagating waves transport heat poleward, no matter what the basic temperature gradient is (Eliassen and Palm, 1961). There is always a heating tendency at higher latitudes and cooling at lower, as a result of flux divergence. Thus, the low-latitude warming cannot be a direct result of planetary wave enhancement. The poleward heating effects force zonal mean in an upward motion at higher latitudes

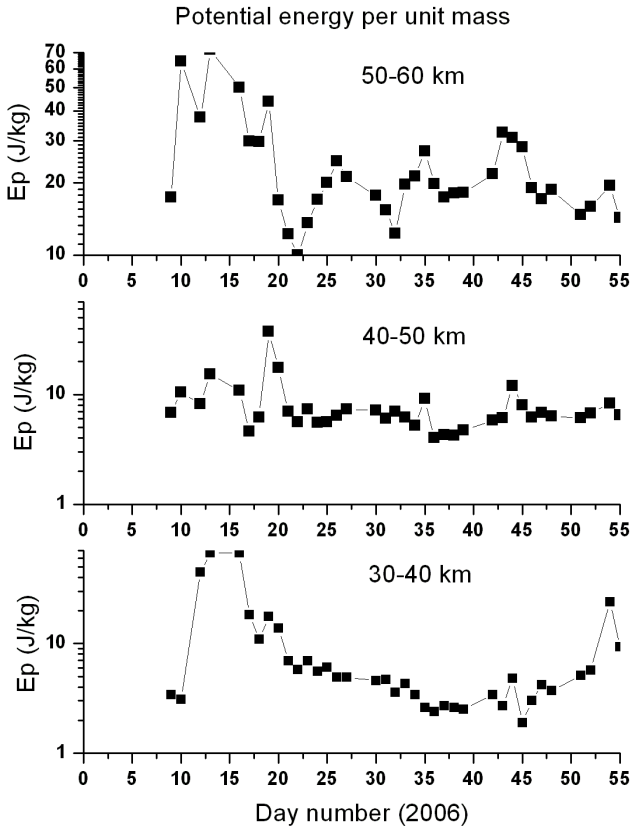

Fig. 4. Time series of potential energy per unit mass in the 30–40 km, 40–50 km and 50–60 km region computed from Rayleigh lidar temperature fluctuations over Gadanki.

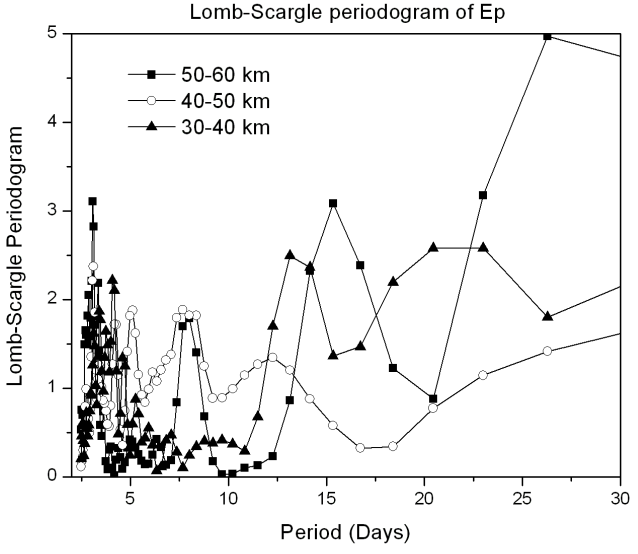

Fig. 5. Lomb-Scargle periodogram of potential energy per unit mass averaged for height regions 30–40 km (curve with triangles), 40–50 km (curve with circles) and 50–60 km (curve with solid squares) over Gadanki.

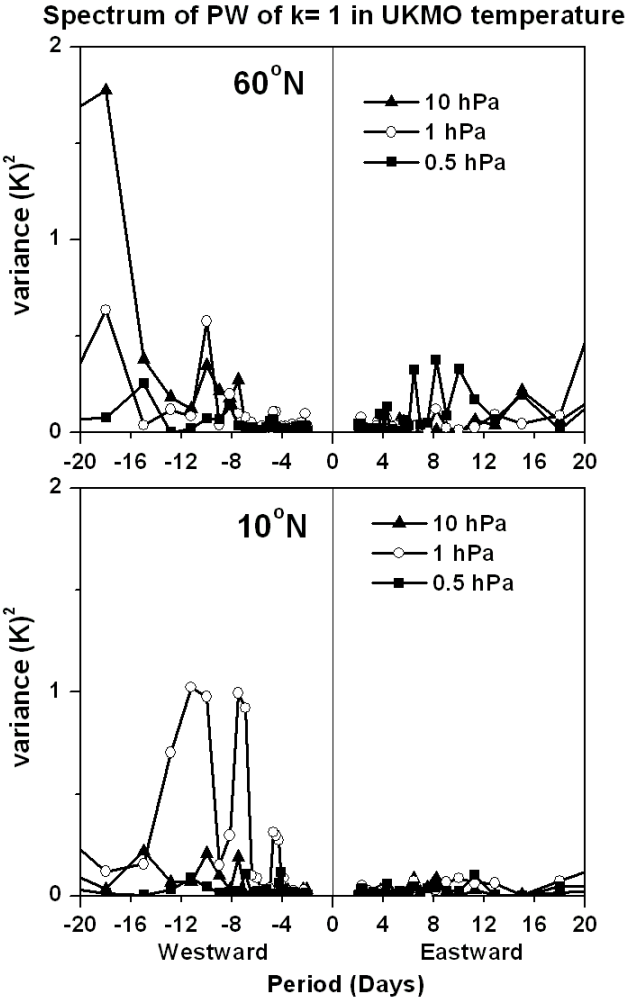

Fig. 6. Spectrum of planetary waves of zonal wavenumber 1 in UKMO temperature data at 60° N (top panel) and 10° N (bottom panel).

and a downward motion at lower latitudes. The forced vertical motions diminish above the critical level because the heat transport vanishes there. Then there must be a flow from higher to lower latitudes near the critical level for the continuity of mass flux. The Coriolis force, acting on this wave induced meridional circulation, is the origin of westward winds. These westward winds form the critical level for the upward propagating planetary waves. The temperature change results from the balance between the eddy heating and the effect of the mean vertical motion. Below the critical level, the former effect exceeds the latter and hence warming occurs at high latitudes. Above the level, only vertical motion causes temperature changes. The zonal mean upward motion above the critical level causes cooling and downward motion at lower latitudes causes warming.

At high latitudes, Whiteway and Carswell (1994) observed greater dissipation of gravity wave energy within the upper

stratospheric warming at high latitudes in comparison with the preceding and following periods. Though the present study reports larger gravity wave activity over Gadanki preceding the period of stratospheric warming, there is no significant increase of gravity wave after the end of the major warming event at high latitude. They also undergo large day to day variability during the observation period and the variabilities are in the time-scale of planetary waves observed in the UKMO temperatures. Hence, additional observations preceding, during and after the future major warming events are required to confirm this behaviour.

Acknowledgements. The authors are grateful to the UKMO and the BADC for the access to the data on http://www.badc.rl.ac.uk/data/assim. NCEP Reanalysis data provided by the NOAA/OAR/ESRL PSD, Boulder, Colorado, USA, from their website at http://www.cdc.noaa.gov.

Topical Editor U.-P. Hoppe thanks one anonymous referee for her/his help in evaluating this paper.

References

Andrews, D. G., Holton, J. R., and Leovy, C. B.: Middle Atmosphere Dynamics, Acad. Press, 1987.

Appu, K. S.: On Perturbations in the Thermal structure of Tropical stratosphere and Mesosphere in Winter, Indian J. Radio Space Phys., 13, 35–41, 1984.

Bhavani Kumar, Y., Siva Kumar, V., Rao, P. B., Krishnaiah, M., Mizutani, K., Aoki, T., and Yasui, Itabe.: Middle atmospheric temperature measurements using ground based instrument at a low latitude, Indian J. Radio Space Phys., 29, 249–257, 2000.

Delisi, D. P. and Dunkerton, T. J.: Seasonal variation of the semiannual oscillation, J. Atmos. Sci., 45, 2772–2787, 1988.

Duck, T. J., Whiteway, J. A., and Carswell, A. I.: Lidar observations of gravity wave activity and arctic stratospheric vortex core warming, Geophys. Res. Lett., 25, 2813–2816, 1998.

Dunkerton, T. J. and Butchart, N.: Propagation and selective transmission of internal gravity waves in a sudden warming, J. Atmos. Sci., 41, 1443–1460, 1984.

Dunkerton, T. J., Delisi, D. P., and Baldwin, M. P.: Distribution of major stratospheric warmings in relation to the quasi-biennial oscillation, Geophys. Res. Lett., 15, 136–139, 1988.

Eliassen, A. and Palm, E., On the transfer of energy in stationary mountain waves, Geofys. Publikasjoner, 12, 1–23, 1961.

Hauchecorne, A. and Chanin, M. L.: Mid latitude observations of planetary waves in the middle atmosphere during the winter over 1981–1982, J. Geophys. Res., 88, 3843–3849, 1983.

Hauchecorne, A. and Chanin, M. L.: Density and temperature profiles obtained by lidar between 35 and 70 km, Geophys. Res. Lett., 8, 565–568, 1980.

Hoffmann, P., Singer, W., Keuer, D., Hocking, W. K., Kunze, M., Murayama, Y.: Latitudinal and longitudinal variability of mesospheric winds and temperatures during stratospheric warming events, J. Atmos. Sol.-Terr. Phys., 69, 2355–2366, 2007.

Holton, J. R.: The influence of gravity wave breaking on the general circulation of the middle atmosphere, J. Atmos. Sci., 40, 2497–2507, 1983.

Kalnay, E., Kanamitsu, M., and Kistler, R.: The NCEP/NCAR 40-year reanalysis project, B. Am. Meteorol. Soc., 77, 437–470, 1996.

Labitzke, K. and Naujokat, B.: The lower Arctic stratosphere in winter since 1952, SPARC Newsletter, 15, 11–14, 2000.

Lindzen, R. S.: Turbulence and stress owing to gravity wave and tidal breakdown, J. Geophys. Res., 86, 9707–9714, 1981.

Matsuno, T.: A dynamical model of the stratospheric sudden warming, J. Atmos. Sci., 28, 1479–1494, 1971.

O'Neill, A. and Pope, V. D.: Simulations of linear and non-linear disturbances in the stratosphere, Q. J. Roy. Meteoral. Soc., 114, 1063–1110, 1988.

Parameswaran, K., Rajeev, K., Sasi, M. N., Geetha Ramkumar, and Krishna Murthy, B. V.: First observational evidence of the modulation of gravity wave activity in the low latitude middle atmosphere by equatorial waves, Geophys. Res. Lett., 29, 6, doi:10.1029/2001GL13625, 2002.

Schoeberl, M. R.: Stratospheric warmings: observations and theory, Rev. Geophys. Space Phys., 16, 521–538, 1978.

Shepherd, T. G.: The middle atmosphere, J. Atmos. Solar. Terr. Phys., 62, 187–1601, 2000.

Siva Kumar, V., Bhavani Kumar, Y., Raghunath, K., Rao, P. B., Krishnaiah, M., Mizutani, K., Aoki, T., Yasui, M., and Itabe, T.: Lidar measurements of mesospheric temperature inversion at a low latitude, Ann. Geophys., 19, 1039–1044, 2001, http://www.ann-geophys.net/19/1039/2001/.

Sivakumar, V., Morel, B., Bencherif, H., Baray, J. L., Baldy, S., Hauchecorne, A., and Rao, P. B.: Rayleigh lidar observation of a warm stratopause over a tropical site, Gadanki (13.5° N; 79.2° E), Atmos. Chem. Phys., 4, 1989–1996, 2004, http://www.atmos-chem-phys.net/4/1989/2004/.

Swinbank, R. and O'Neill, A.: A stratosphere–troposphere data assimilation system, Mon. Weather Rev., 122, 686–702, 1994.

Swinbank, R. and Ortland, D. A.: Compilation of wind data for the Upper Atmosphere Research Satellite (UARS) Reference Atmosphere Project, J. Geophys. Res., 108(D19), 4615, doi:10.1029/2002JD003135, 2003.

Walterschied, R. A., Sivjee, G. G., and Roble, R. G.: Mesospheric and lower thermosphere manifestations of a stratospheric warming event over Eureka, Canada (80° N), Geophys. Res. Lett., 27, 2897–2900, 2000.

Whiteway, J. A. and Carswell, A. I.: Rayleigh lidar observations of thermal structure and gravity wave activity in the high arctic during a stratospheric warming, J. Atmos. Sci., 51, 3122–3136, 1994.

Whiteway, J. A., Duck, T. J., Donovan, D. P., Bird, J. C., Pal, S. R., and Carswell, A. I.: Measurements of gravity wave activity within and around the Arctic stratospheric vortex, Geophys. Res. Lett., 24, 1387–1390, 1997.